Nanometer-Scale Vibration
in Mutant Axonemes of *Chlamydomonas*

クラミドモナス突然変異株鞭毛におけるナノメートルスケール高速振動

名古屋大学大学院理学研究科

八木　俊樹

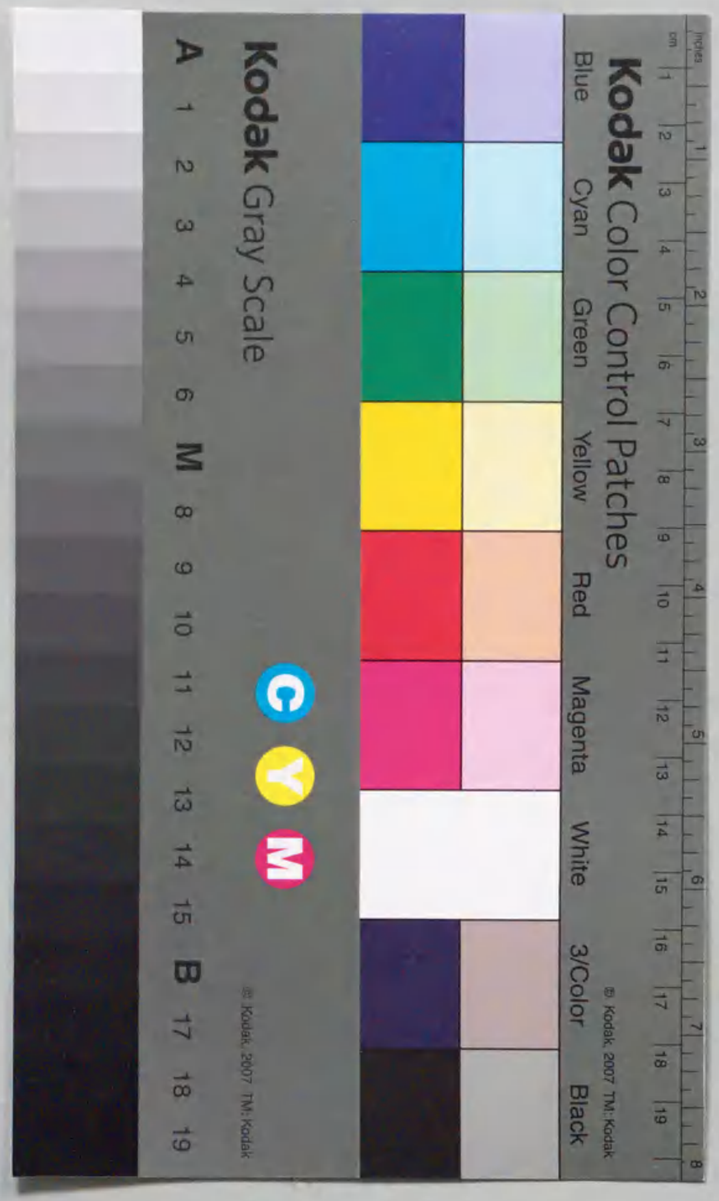

(1)

Nanometer–Scale Vibration in Mutant Axonemes of *Chlamydomonas*

Toshiki Yagi

Department of Molecular Biology

Graduate School of Science, Nagoya University

February, 1995

SUMMARY

Flagellar axonemes of sea urchin sperm is known to display high frequency (200–400 Hz) vibration (hyper–oscillation) with nanometer–scale amplitudes in the presence of ATP. To investigate whether the vibration also occurs in axonemes from other organisms and how various axonemal components affect the vibration, I examined vibration in wild–type and mutant axonemes of *Chlamydomonas*. At 1 mM ATP, wild–type axonemes underwent vibration at 100–650 Hz with amplitudes of 4–40 nm. This vibration was similar to, but less regular than, that in sea urchin sperm. Axonemes of the mutants *ida1* and *ida4* lacking part of the inner–arm dynein underwent vibrations indistinguishable from that of wild type. The mutant *oda1* lacking the entire outer arm underwent vibration at about half the wild–type frequency. Unexpectedly, the paralyzed mutants *pf18* lacking the central pair and *pf14* lacking the radial spokes displayed vibration with significantly higher frequencies and smaller amplitudes than those in the wild–type vibration. These results indicate that the high–frequency vibration is common to many kinds of mutant axonemes that lack various axonemal substructures, but that its manner is sensitive to the presence of outer–arm dynein and the central pair/radial spoke system. Simultaneous measurements of amplitude and frequency in wild–type and mutant axonemes suggest that the velocity of microtubule sliding in vibrating axonemes is lower than the velocity of sliding under load–free conditions. The velocity is particularly low in *pf18*. A possible mechanism is proposed to explain the lower sliding velocity and vibration amplitude in the *pf18* axoneme, based on an assumption that central pair/radial spoke system may work to regulate the switching of two antagonizing forces within the axoneme.

The *pf18* axoneme has recently been found to display an undulating movement in the simultaneous presence of ATP and ADP. I found that the amplitude of hyper–oscillation increases significantly under the condition where the mutant axoneme can undulate. The hyper–oscillation under these conditions often takes on an exceptionally simple asymmetric pattern, in which the maximal shearing velocity exceeds 50 μm/sec, much higher than the maximal velocity in ordinary dynein–microtubule sliding. It thus appears that the asymmetric oscillation is

brought about by a combination of an active force produced by dynein and an internal elastic force. The amplitude of this oscillation can be as large as 0.1 μm, suggesting that the elastic component can be stretched up to 0.1 μm. Analyses of these patterns prompt us to speculate that axonemal dyneins have a tendency to attach to and detach from doublets cooperatively and that the mechanochemical cycle of dynein has an inherent refractory period of about 2 msec, during which dynein cannot interact with microtubules. These properties should be important in considering the mechanism of axonemal beating.

INTRODUCTION

The beating of cilia and flagella is a result of inter–doublet sliding driven by dynein arms [Gibbons, 1981]. The oscillatory movement of an axoneme with a regular waveform must be produced by controlled activation and inactivation of specific dynein arms, but the mechanism for this control has been unknown. Currently prevailing theories postulate that the activity of dynein arms is controlled by the mechanical state of axoneme, such as curvature, which in turn is determined by the activity of dynein arms; axonemes oscillate because of this feedback [Brokaw, 1985]. However, it remains possible that dynein arms have an intrinsic tendency to oscillate, and this nature of dynein somehow gives rise to the beating movement of the axoneme [Brokaw, 1990].

In this respect, the high–frequency vibration recently found by Kamimura and Kamiya [1989, 1992] in sea urchin sperm axonemes appears to be an important phenomenon that may be the manifestation of the oscillatory nature of dynein. Using an optical device designed to detect nanometer–scale movements, they found a new motility phenomenon in sea urchin sperm flagellar axonemes: a nanometer–scale, high–frequency vibration that occurs as back–and–forth shearing between two groups of outer doublets within an axoneme. Its shear amplitude, 4–30 nm, is more than ten times smaller than that in the ordinary flagellar beating and its frequency, 200–400 Hz at 1 mM ATP, is more than ten times higher than that in the normal beating. The frequency was variable with ATP concentration in a manner consistent with Michaelis–Menten kinetics with an apparent Km similar to that obtained for the beat frequency in reactivated axonemes. It is inhibited by vanadate, a potent inhibitor of dynein ATPase. Furthermore, its shear amplitude takes discrete values of 4, 12, 20, 28, 36, $\cdots$ nm, which are combinations of the size of a tubulin monomer (4 nm) and a dimer (8 nm). These properties indicate that the vibration reflects the interaction between dynein and microtubules at a molecular level, and thus its analysis may yield new information about the dynein–microtubule interaction as well as about the mechanism of flagellar beating [see Brokaw, 1990; Murase, 1992].

To assess the contribution of various axonemal components (see Fig. 1) to the vibration,

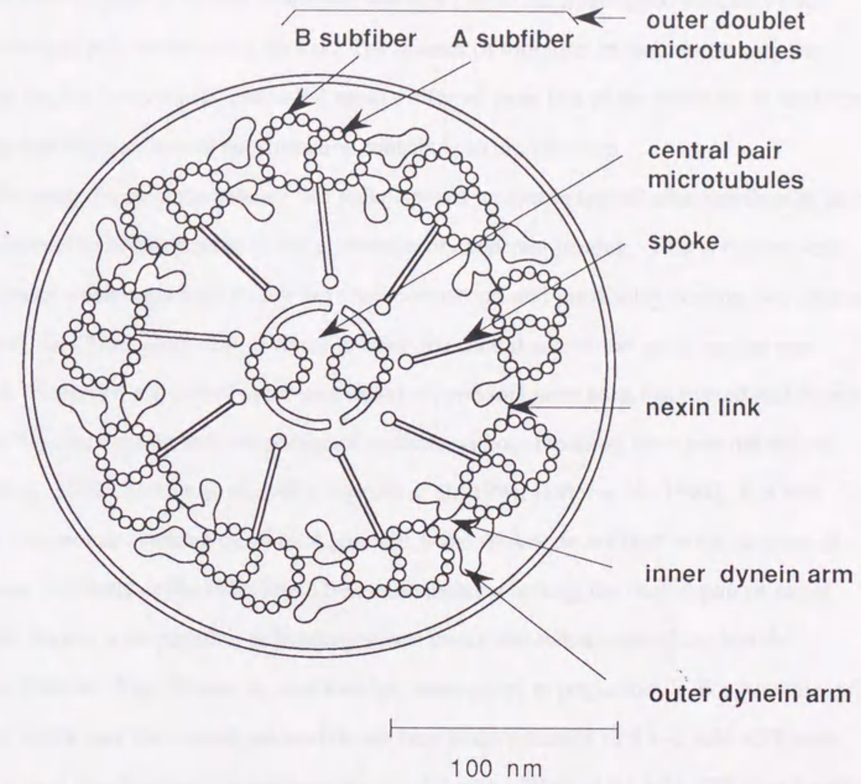

Fig. 1. Diagram of the *Chlamydomonas* flagellum in cross section.

this study examined high-frequency vibration in axonemes of *Chlamydomonas*, of which a number of mutants lacking discrete flagellar components are available. I found that the vibration occurs in wild-type axonemes in a manner similar in many respects to that in sea urchin sperm. Vibration also occurred in mutant axonemes that lack part of the inner arms, the entire outer arms, the central pair, or the radial spokes. The manner of vibration in mutants lacking the outer-arm dynein, central pair, and radial spokes differed from that of the vibration in wild type, indicating that these axonemal substructures contribute to the vibration.

The central-pair microtubules and radial spokes present in typical cilia and flagella have been considered to be unessential to the generation of axonemal beating. This is because cilia and flagella of some organisms do not have these structures and yet display beating [see Ishijima et al, 1988]. In *Chlamydomonas*, mutants missing the central pair or the radial spokes are paralyzed. However, a group of mutations called suppressors have been discovered and shown to restore flagellar beating in these paralyzed mutants without repairing the structural defects [Huang et al., 1982; Brokaw et al., 1982; Piperno et al., 1994; Porter et al., 1994]. It is thus puzzling why mutants lacking the central pair and radial spokes do not beat in the absence of suppressors. Recently, it has been found that these mutants lacking the central pair or radial spokes can display a propagation of bending waves under somewhat unusual nucleotide conditions [Omoto, Yagi, Kurimoto, and Kamiya, manuscript in preparation]. For example, *pf18* axonemes which lack the central pair and do not beat in the presence of 0.1–1 mM ATP were found to beat at low frequency in the presence of 0.02 mM ATP or of 0.1 mM ATP plus 1 mM ADP. I examined the hyper-oscillation in *pf18* axonemes while changing the ADP concentration, and found that the increase in ADP concentration results in a significant increase in amplitude of hyper-oscillation. This result suggests that the central pair/radial spoke system in a normal axoneme has a function to increase the shear amplitude. Furthermore, I found that the oscillation at high ADP concentrations often took on an extremely simple asymmetric patterns. This novel pattern of beating seems to suggest the presence of an internal elastic component that can be stretched as much as 0.1 μm, cooperative attachment/detachment of

dynein arms, and a refractory period during which dynein cannot attach to outer doublet. These implications should be important in considering the mechanism of flagellar motility in general.

MATERIALS AND METHODS

Strains

Chlamydomonas reinhardtii 137c (wild type (*wt*); mating type + and −) and the following flagellar mutants were used: *ida1* and *ida4* lacking different subspecies of inner−arm dyneins [Kamiya et al., 1991], *oda1* lacking the entire outer dynein arm [Kamiya, 1988], *pf18* lacking the central−pair microtubules, and *pf14* lacking the radial spokes [see Harris, 1988].

Culture of Cells and Isolation of Axonemes

Cells were grown in 200 ml of Tris−acetate−phosphate (TAP) medium [Gorman and Levine, 1965] with aeration over a 12 h/12 h, light/dark cycle. Flagella were obtained by the method of Witman et al.[1978], using dibucaine−HCl to detach flagella from the cell bodies. The isolated flagella were collected by centrifugation and demembranated to axonemes in HMDEKP [30 mM Hepes (pH 7.4), 5 mM $MgSO_4$, 1 mM dithiothreitol (DTT), 1 mM EGTA, 50 mM K−acetate and 1% polyethylene−glycol (PEG 20,000 mol wt)] containing 0.2% Nonidet P−40.

Detection of Vibration

The motion of polystyrene microbeads (diameter about 1 μm; Polyscience Co., Warrington, PA) attached to an axoneme was monitored with a sensitive optical detector. Axonemes were introduced into a flow−chamber made of a cover slip and a glass slide (Matsunami No. 0) held with a pair of cover slip strips. After a few minutes, the flow−chamber was perfused with HMDEKP to wash out the axonemes that did not attach to the glass surface. Microbeads were then attached to the axonemes by perfusing the chamber with a 0.05% (w/v) suspension in HMDEKP. A small fraction of the microbeads became attached to the axonemes within a few minutes. Microbeads not attached were washed out with HMDEKP. In typical experiments with wild−type axonemes, high−frequency vibration occurred, upon perfusion with HMDEKP containing ATP, in about one half of the axonemes to which microbeads were attached. When the effect of ATP concentration was examined, an ATP regeneration system

with 70 units/ml of creatine phosphokinase and 5 mM creatine phosphate, made in HMDEKP, was used. The vibration continued for more than 30 minutes under usual experimental conditions, allowing us to follow the change in the vibration of a single microbead while changing solution conditions.

The signal of high-frequency vibration usually contained noise resulting from mechanical vibration of the equipment and thermal fluctuation of the sample, making it difficult to measure the amplitude of regular vibration. Therefore, when the amplitude was measured, the cover slip was coated with poly-L-lysine (P-1524, Sigma) so as to firmly attach the axoneme.

Apparatus for Observation

The apparatus used to detect nanometer-scale vibration was constructed essentially after Kamimura and Kamiya [1992]. The apparatus constructed in S.K.'s laboratory and used in the previous study was also used in some experiments to confirm that essentially the same results are obtained with the two apparatuses. The new apparatus consisted of a microscope (BH-2, Olympus, Tokyo) and an optical detector with a quadrant-type photodiode (S1557, Hamamatsu Photonics, Hamamatsu, Japan) (Fig. 2a). The entire apparatus was placed on an air-damping table (AFM-1007, Meiritsu-Seiki Co., Tokyo). The quadrant-type photodiode was mounted on an X-Y stage placed on the back-focal plane of the eyepiece. This X-Y stage and the microscope specimen stage were adjusted so that the image of a microbead was projected on the central area of the diode. The photocurrent from the four quadrants were fed into differential amplifiers, the output of which yielded information regarding the relative position of the microbead (Fig. 2b). The output was filtered through a low-pass filter (cutoff frequency: 1 or 2 kHz), monitored with an oscilloscope, and recorded with a digital-audio-tape (DAT) recorder (SV-DA10, Panasonic, Osaka, Japan). The frequency spectrum of the vibration was obtained with an FFT analyzer (AD-3524, A and D Co., Tokyo). For measuring the amplitude of vibration, the digital output from the FFT analyzer was transferred to a personal computer through a GP-IB interface and the peak values of the vibration was detected by a home-made

program. The method used for calibration of the apparatus has been described before [Kamimura and Kamiya, 1992].

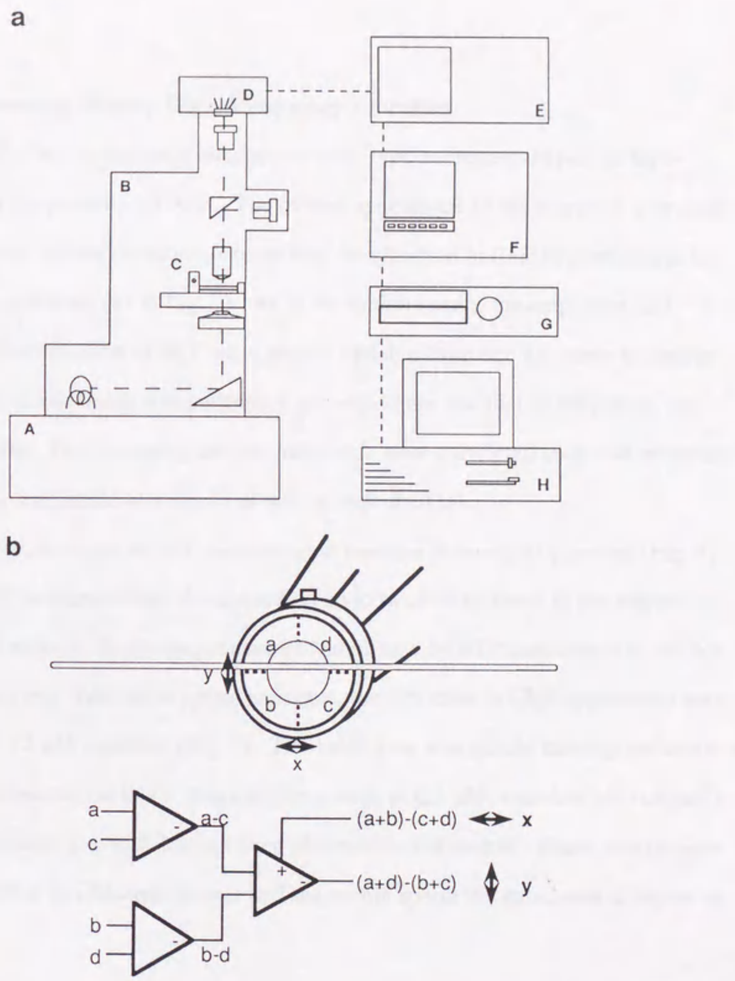

Fig. 2. Diagram (**a**) and circuit (**b**) of the apparatus. (**a**) (**A**) air dumping table; (**B**) microscope; (**C**) piezo actuator for calibration; (**D**) quadrant–type–photodiode; (**E**) digital oscilloscope; (**F**) FFT analyzer; (**G**) digital–audio–tape (DAT) recorder; (**H**) personal computer. (**b**) Schematic diagram of the circuit for the two–dimensional detector. The image of the bead attaching to the axoneme is projected on the detecting plane of the photodiode. The differential operational amplifiers calculate the output of the photodiode into the displacement of the bead in X and Y directions.

RESULTS

Chlamydomonas Axonemes Display High–Frequency Vibration

About one half of the microbeads attached to wild–type axonemes displayed high–frequency vibration in the presence of ATP. The overall appearance of the vibration was similar to that of the vibration in sea urchin sperm, except that the vibration in *Chlamydomonas* is less regular in period and amplitude (*wt* in Fig. 3). As in sea urchin sperm, the amplitude and frequency at a given concentration of ATP were greatly variable from one axoneme to another. The range of variation of amplitude was between 4 nm and 40 nm and that of frequency was between 100 and 650 Hz. The frequency and the amplitude were correlated such that when the frequency was high the amplitude was small, as will be described later.

As in sea urchin, decrease in ATP concentration resulted in lower frequencies (Fig. 4). However, lowered ATP concentrations also caused an up to twofold increase in the vibration amplitude in *Chlamydomonas*. Such a dependence of amplitude on ATP concentration has not been observed in sea urchin. Also as in sperm axoneme, the vibration in *Chlamydomonas* was completely inhibited by 2 μM vanadate (Fig. 5). This inhibition was mainly through reduction in vibration amplitude. However, at lower concentrations such as 0.1 μM, vanadate also caused a 10–30% increase in frequency, which has not been observed in sea urchin. These observations indicate that the vibrations in *Chlamydomonas* and sea urchin sperm are somewhat different in detail.

Vibration in Mutant Axonemes

I found that high–frequency vibration occurs in the mutants *ida1* lacking part of the inner dynein arm, *oda1* lacking the outer dynein arm, *pf18* lacking the central pair, and *pf14* lacking the radial spokes (Fig. 3). It should be noted that the former two mutants are slow–swimmers, whereas the latter two are paralyzed. Hence, flagellar motility itself is not necessary for high–frequency vibration. I have observed vibration also in the mutants *ida4* (slow–swimmer) and *pf*23 (paralyzed) lacking part of the inner–arm dynein, and *pf17* (paralyzed) lacking the spoke

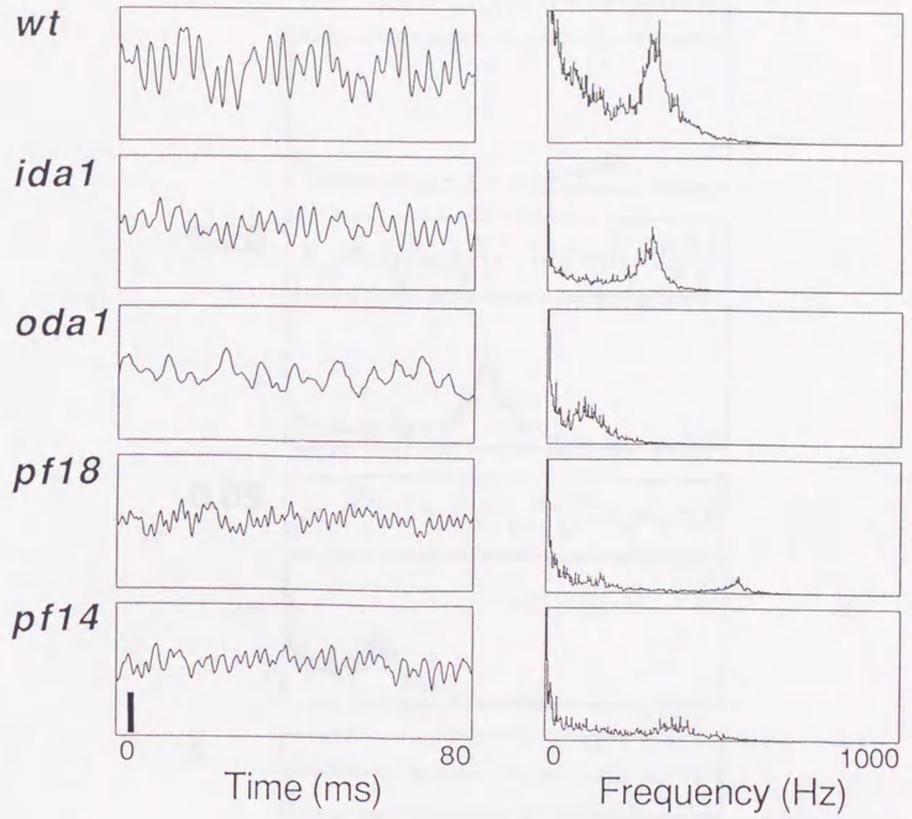

Fig. 3. Examples of high–frequency vibration in wild type and mutants: *ida1* lacking part of the inner–arm dynein, *oda1* lacking the entire outer dynein arm, *pf18* lacking the central pair, and *pf14* lacking the radial spokes. In each sample, the left panel shows a 80 msec record of the direct output from the detector, representing the movement of microbead in the direction of axonemal axis. Bar: 10 nm. The right panel shows the power spectrum of the output, averaged over 4 seconds. Vertical scales are in arbitrary units. ATP concentration: 1 mM. Temperature: 23°C.

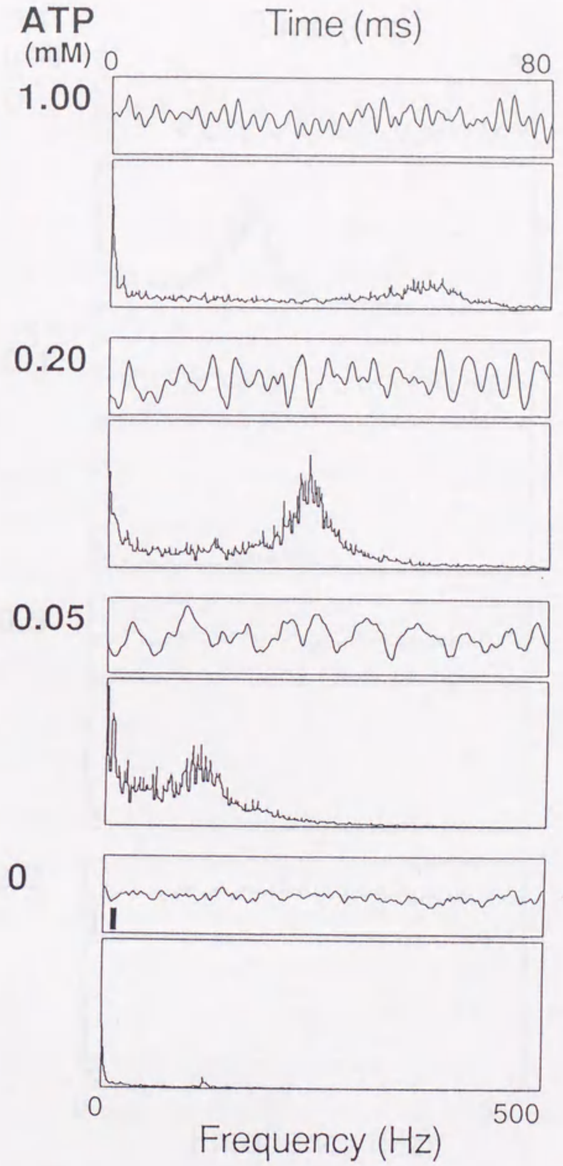

Fig. 4. ATP–dependence of the vibration in wild–type axoneme. Upper and lower panels show the direct output and their power spectra, respectively. ATP concentrations: 1 mM, 0.2 mM, 0.05 mM, and 0 mM. A small peak in the FFT spectrum at 0 mM is due to mechanical noise. An ATP regenerating system was used. Temperature: 23 ° C. Bar: 10 nm.

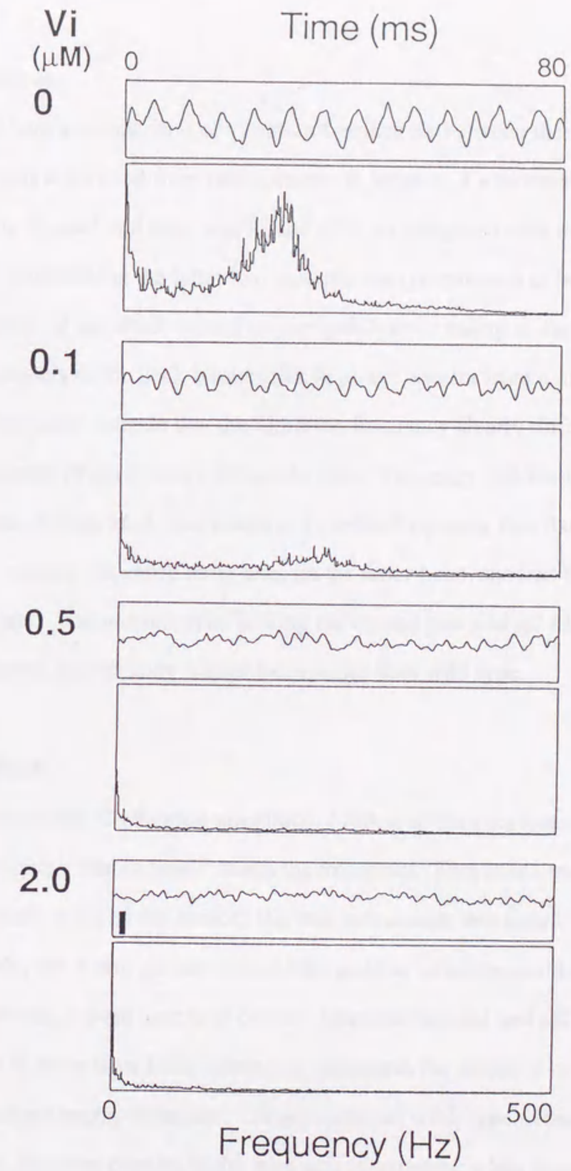

Fig. 5. Inhibition of vibration by vanadate in wild-type axoneme. Upper and lower panels show the direct outputs and their power spectra. Vanadate concentrations: 0 μM, 0.1 μM, 0.5μM, and 2.0 μM. ATP concentration: 1 mM. Temperature: 23°C. Bar: 10 nm.

head (data not shown).

I describe here a comparison of vibration frequencies between these mutants. Although the pattern of vibration differed from one axoneme to another, it was consistently observed that frequency was low in *oda1* and high in *pf18* and *pf14*, as compared with that of wild type. Furthermore, the amplitude in the latter two mutants always appeared to be small, although a precise measurement of amplitude would require polylysine coating of the glass surface (see below). I took statistics of the peak frequencies in power spectra from a number of different samples. The histograms indicate that the vibration frequency clearly differs between mutants (Fig. 6). The axoneme of *ida1* shows almost the same frequency distribution as that of wild type. Another inner-arm mutant, *ida4*, also displays a similar frequency distribution (data not shown). The mutant *oda1* lacking the entire outer arm, on the other hand, showed frequencies about half the wild-type values. The mutants *pf18* lacking the central pair and *pf14* lacking the radial spokes both displayed significantly higher frequencies than wild type.

Vibration Amplitude

For measurements of vibration amplitude, I followed the previous study and coated the glass surface with polylysine to firmly attach the axonemes [Kamimura and Kamiya, 1992]. This treatment greatly reduced the random thermal movements that interfere with the analysis of vibration amplitude, but it also greatly reduced the number of axonemes that underwent vibration. In particular, I were unable to observe vibration in *oda1* and *pf14* with polylysine-coated cover slips in more than 1,000 axonemes examined; the reason is not understood.

Like sea urchin sperm axonemes, *Chlamydomonas* wild-type axonemes were found to vibrate only in the direction parallel to the long axis of axoneme when attached to the polylysine-coated cover slips. Hence, the vibration must occur as a back-and-forth movement between groups of doublets as in sea urchin. Fig. 7A-C show three typical examples of vibration in wild-type axonemes displaying different amplitude distributions. In the measurement of amplitude, I distinguished the two slopes of a wave (arbitrarily called ascending and descending)

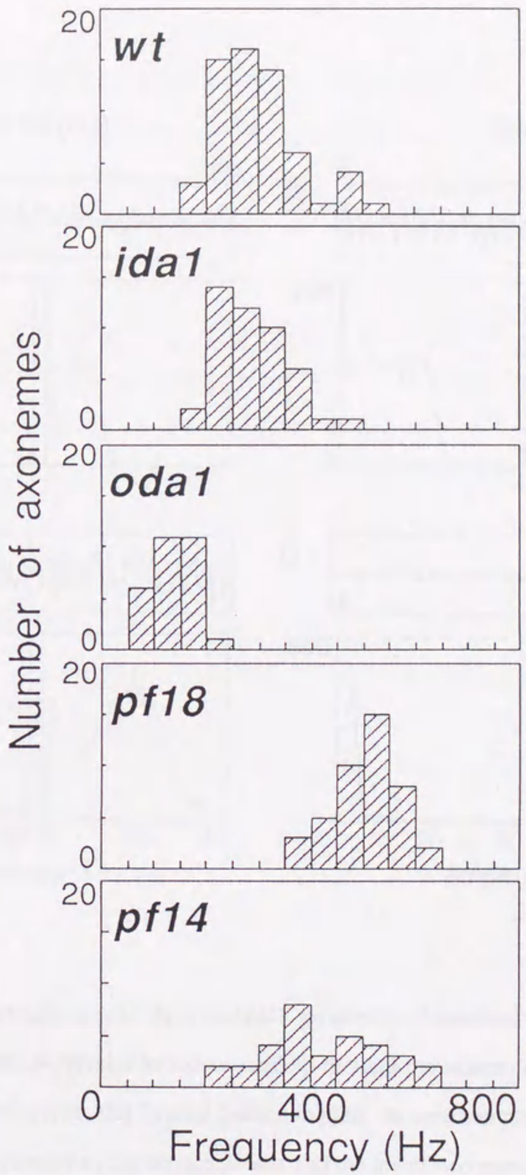

Fig. 6. Histograms of vibration frequencies in wild-type and mutant axonemes. Peak frequencies in the power spectra were measured in > 20 axonemes each of wild type, *ida1*, *oda1*, *pf18*, *pf14*. ATP concentration: 1mM. Temperature: 23 ° C.

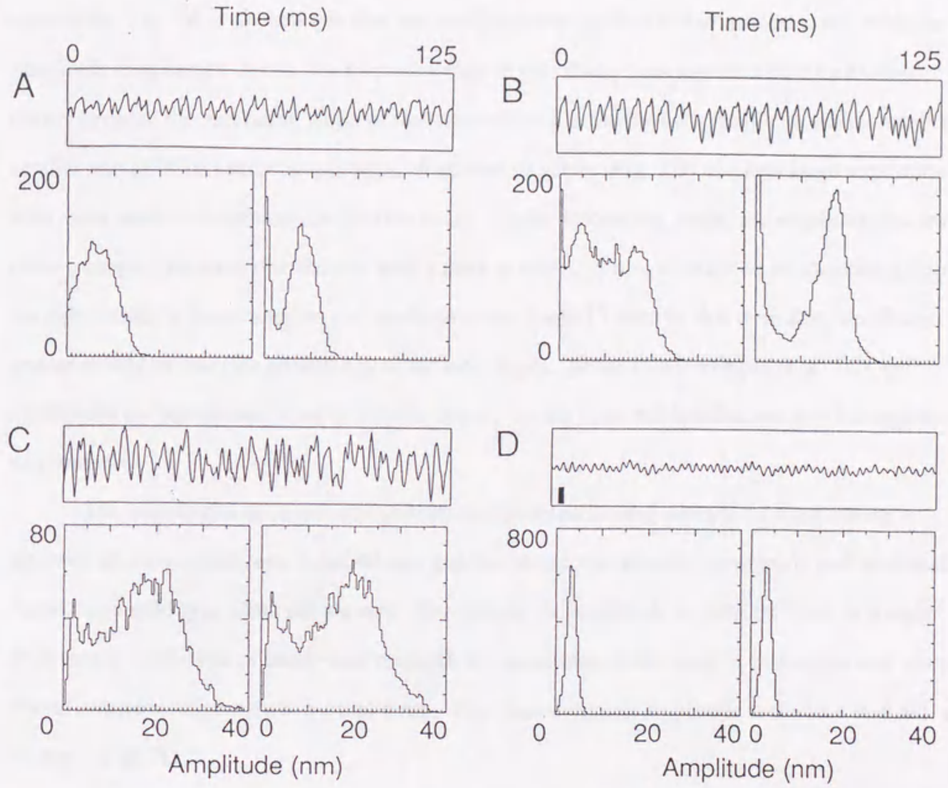

Fig. 7. Vibration amplitude in wild–type and *pf18* axonemes. Axonemes were firmly attached to the glass surface with polylysine to reduce random thermal movement. (**A–C**) Three different types of vibration in wild type. (**D**) Typical pattern in *pf18*. In each sample, the upper panel shows the movement parallel to the axonemal axis and the lower two panels show the histograms of peak–to–peak amplitudes in ascending and descending slopes, respectively. ATP concentration: 1 mM. Temperature: 23 °C. Bar: 10 nm.

because most axonemes adsorbed on the polylysine–coated glass surface displayed asymmetric vibrations. Fig. 7A is an example that has small amplitudes distributed around 8 nm, with the amplitude distribution in one slope broader than in the other. This asymmetric distribution occurs because the ascending slope of this wave often has one or two shoulders, which result in smaller values of measured amplitudes. A second example (Fig. 7B) displays large amplitudes with more marked asymmetry in the two slopes. In its descending slope, the amplitude values show a simple Gaussian distribution with a peak at about 18 nm, whereas in its ascending slope the distribution is broad and has two peaks at about 5 and 17 nm. In this case also, shoulders appear mostly in one (the ascending) of the two slopes. In the third example (Fig. 7C), the amplitudes are distributed broadly in both slopes. In this case the distribution may be regarded as symmetric.

The amplitudes at the peak in distribution patterns in *ida1* and *ida4* varied among different axonemes between 4 and 40 nm, and the waveform assumes symmetric and asymmetric forms, as in wild type (data not shown). In contrast, the amplitude in *pf18* differed strikingly from that in wild–type or inner–arm mutants: the amplitude at the peak in histogram was always within a narrow range between 3 and 6 nm. The most common amplitude was close to 4 nm, as shown in Fig. 7D.

Measurements of the amplitude and frequency in many samples revealed a reciprocal relationship between these values; i.e., the lower the amplitude, the higher the frequency. Fig. 8 shows the plots of the amplitudes at the peaks in histograms against the frequencies at the peaks in the power spectra measured in wild–type and mutant axonemes. [When multiple peaks were present in an amplitude histogram, I chose the value of the highest peak as the amplitude. For example, I adopted 18 nm as the amplitude value in Fig. 7B]. Although the plots show a significant scatter, the data for wild type, *ida1*, and *ida4* are similarly distributed, confirming the above–mentioned observation that the vibration in inner–arm mutants is similar to that in wild type in amplitude as well as in frequency. On the other hand, the plots for the *pf18* axoneme differ significantly from those of the other three kinds of axonemes. The plots for *pf18*

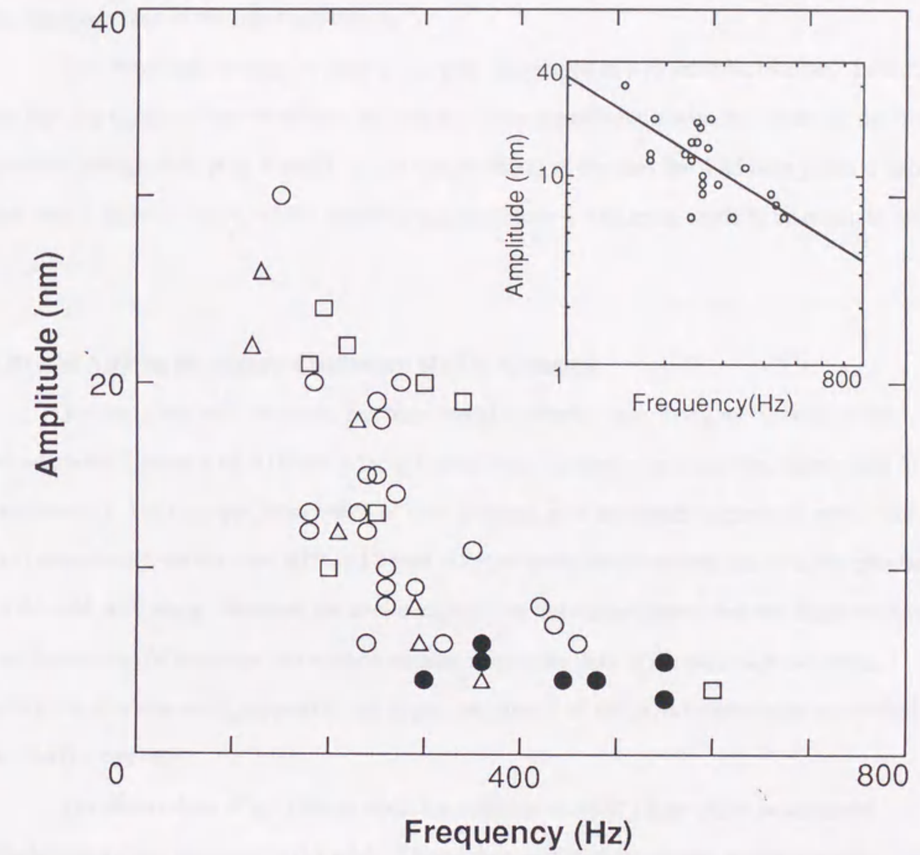

Fig. 8. Plots of the amplitude against frequency in wild type and mutants. The amplitude at the peak in amplitude histograms and the peak frequency in power spectra are plotted for different axonemes. Samples measured are wild type (open circles), *ida1* (open triangles), *ida4* (open squares), and *pf18* (filled circles). When more than two peaks appeared in an amplitude histogram, the largest one was adopted for the peak amplitude. The numbers of data are 23 for wild type, 7 for *ida1*, 8 for *ida4* and 7 for *pf18*. (Inset) Double logarithmic plots of the data for wild type. The linear line is a least square regression line, which has a slope of −1.04, indicating that frequency x amplitude tends to be constant (3.2 μm/sec).

axonemes are restricted to the lower end of the distribution, with significantly smaller variation in amplitude than in the other axonemes.

The amplitude–frequency data are largely distributed in a hyperbolic manner. In fact, if the data for wild–type axonemes are plotted in double logarithmic scales, the plots are distributed around a straight line (Fig. 8 inset). Least square fitting of the data for wild type yields a linear line with a slope of −1.04, which suggests that amplitude x frequency tends to be constant (about 3.2 μm/sec).

Effect of ADP on the Hyper–Oscillation of *pf18* Axoneme

Recently, the *pf18* axoneme has been found to display undulating movements in the simultaneous presence of ATP and ADP [Omoto, Yagi, Kurimoto and Kamiya, manuscript in preparation]. For example, about 40% of free–floating *pf18* axonemes underwent undulation in the presence of both 0.1 mM ATP and 3 mM ADP, whereas no axonemes did so in the presence of 0.1 mM ATP alone. Because the above experiment has demonstrated that the high–frequency oscillation in *pf18* axoneme has a much smaller amplitude than in the wild type axoneme, I wanted to examine what happens to the hyper–oscillation of the *pf18* axoneme under conditions in which it can beat.

For observation of the change upon the addition of ADP, I first chose an axoneme displaying regular vibration at 0.1 mM ATP and then perfused the sample with a solution containing ATP plus ADP while observing the identical axoneme. Although many axonemes stopped vibration during the perfusion, I were able to observe about 20 axonemes that revealed the effects of the ADP addition.

The vibration amplitude almost always increased upon the addition of ADP, although the degree of the increase differed from an axoneme to another. The pattern of the vibration curve in the presence of ADP differed significantly among axonemes, but there appeared to be two general types. The first type, as shown in Fig. 9a, is a somewhat irregular pattern in which the slopes of the curve in both directions show similar changes; the movement of the microbead can

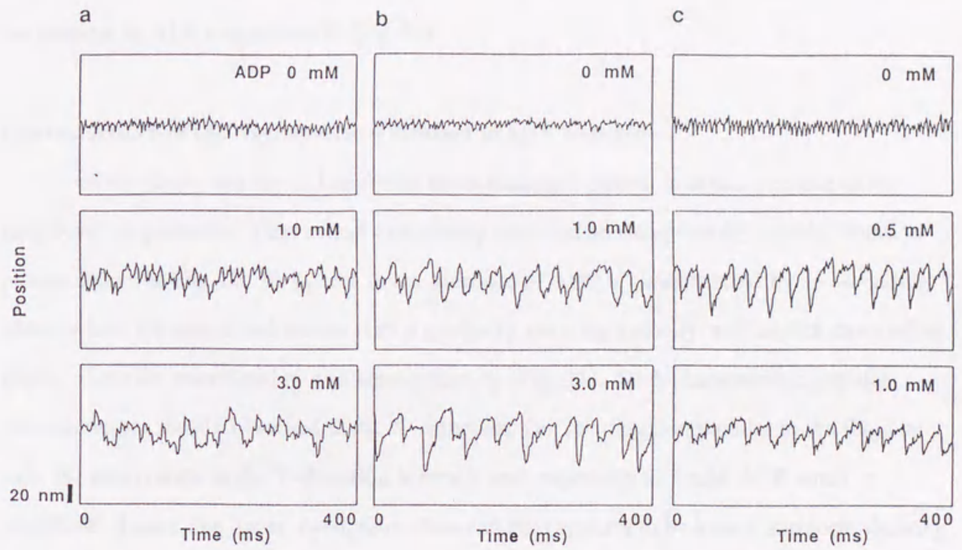

Fig. 9. Effect of ADP on the hyper–oscillation of *pf18* axoneme. Axonemes undergoing hyper–oscillation in 0.1 mM ATP were perfused with a solution containing 0.1 mM ATP and the indicated concentration of ADP. (**a**) axoneme that shows an irregular but fairly symmetrical pattern. (**b**) and (**c**) examples that show highly asymmetric patterns in the presence of ADP. Temperature; 25 ° C.

be regarded symmetric in this case. About 70% of the axonemes examined displayed this pattern. The second pattern, as shown in Fig. 9b and 9c, is strikingly asymmetric; the microbead moves in different directions at significantly different speeds, thus giving rise to an asymmetric pattern. This pattern accounts for the rest of the records. In most cases, the amplitude increased with the ADP concentration. Sometimes, however, amplitude increased and then decreased with the increase in ADP concentration (Fig. 9c).

Characteristics of the Asymmetric Vibration in *pf18* Axoneme

Of the above two types, I analyzed the asymmetric pattern in detail, because of its simplicity. In particular, I have most extensively analyzed an exceptionally simple vibration pattern shown in Fig. 10. Its pattern in the presence of ADP is characterized by an ascending phase, where the microbead moves with a gradually lowering velocity, and a quick descending phase, where the microbead moves almost linearly (Fig. 11). Such characteristic, regular movements are mostly observed in the X–direction, i.e., the direction parallel to the flagellar axis; the movements in the Y–direction is erratic and, especially at 3 mM ADP, small in amplitude. Hence, the hyper–oscillation observed here appears to be a back and forth shearing movements between outer doublets, although the shear amplitude is much greater than that of the hyper–oscillation observed before.

Because the descending phase is almost linear in many cases, I can easily measure the velocity and amplitude in this phase. Such measurements indicate that both amplitude and velocity increase with the ADP concentration; the maximal amplitude is about 110 nm and the maximal velocity is about 60 μm/sec (Fig. 12). The plots also show that the velocity is almost proportional to the amplitude, and that the proportion coefficient is almost identical for three different nucleotide conditions. Since the velocity was calculated by dividing the amplitude by the time period (dt) of the descending phase, this result should mean that the duration of the descending phase is almost constant irrespective of the ADP concentration. Direct measurements of dt in the records showed that dt varied only slightly with the ADP

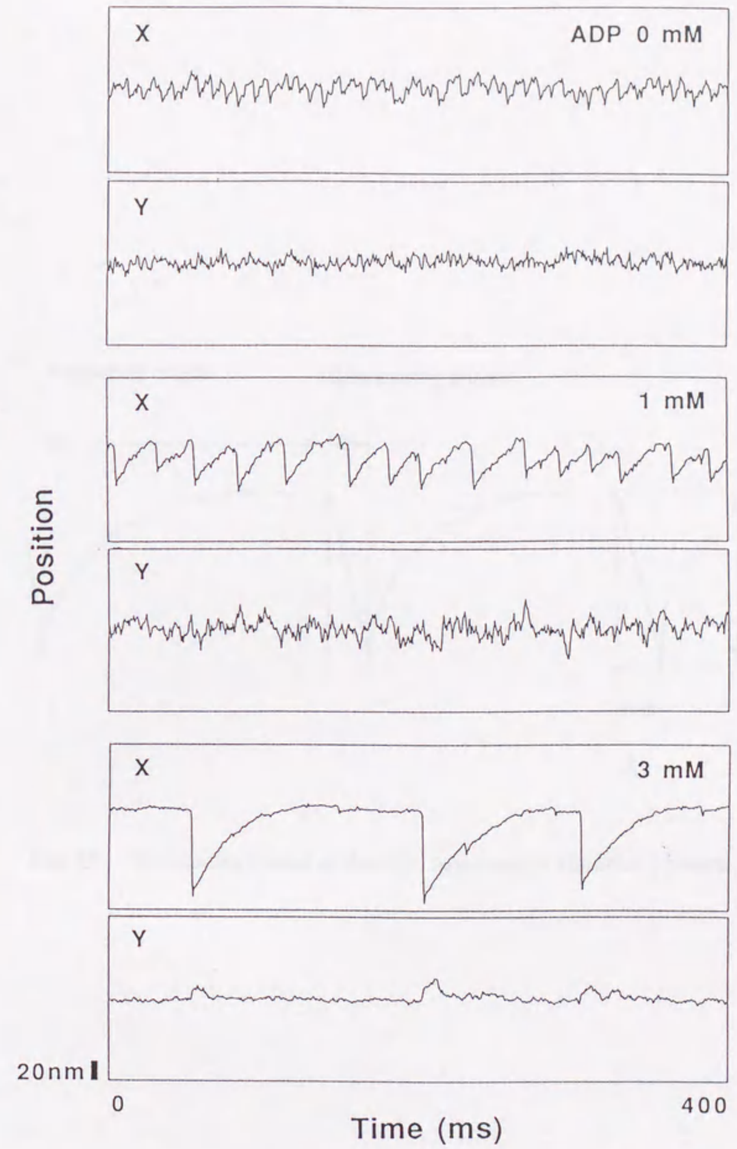

Fig. 10. An example that showed a strikingly simple pattern. The upper panel at each concentration of ADP shows the movements parallel to the flagellar axis; the lower panel shows movements perpendicular to it. Experimental conditions are the same as in Fig. 9.

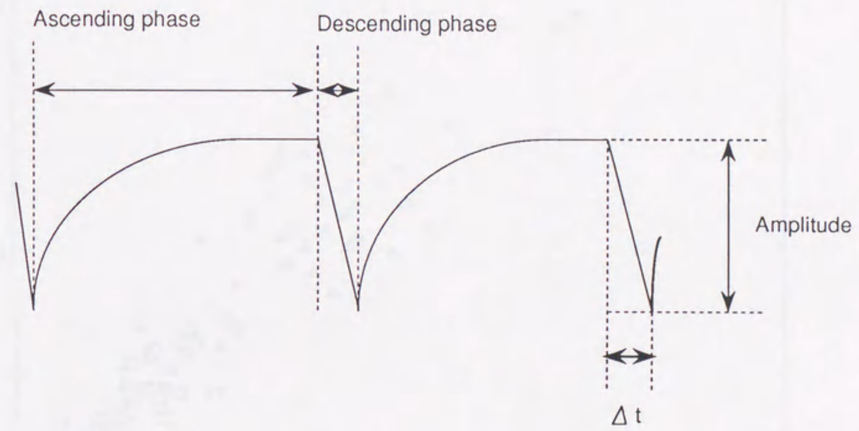

Fig. 11. Terminology used to describe asymmetric vibration patterns.

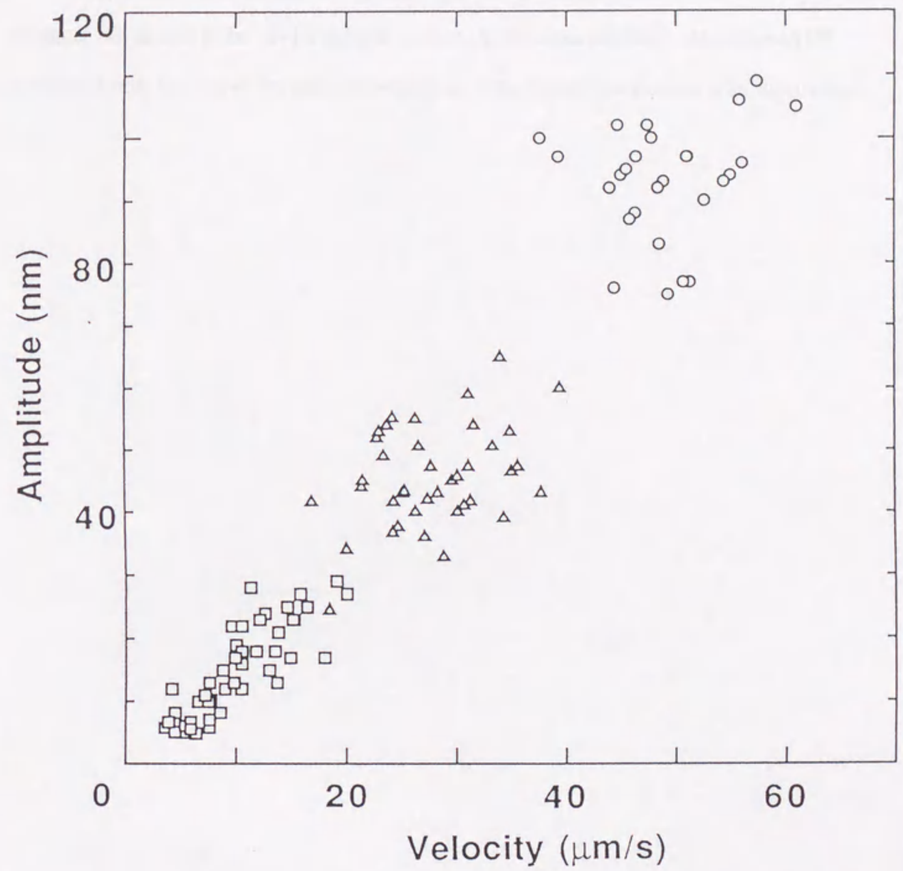

Fig. 12. Relationship between the amplitude and velocity of the movements in the quick descending phase in Fig. 10. ATP: 0.1mM. Squares, no ADP; triangles, 1mM ADP; circles, 3mM ADP. Note that the two quantities are roughly proportional.

concentration: 1.56 msec at 0 mM and 1.93 msec at 3 mM (Fig. 13).

In the ascending phase, the velocity gradually lowers. The initial velocity is difficult to estimate, but seems to be 8–15 μm/sec at each ADP concentration. At higher ADP concentrations, the curve became smoother, as if backward movement was suppressed.

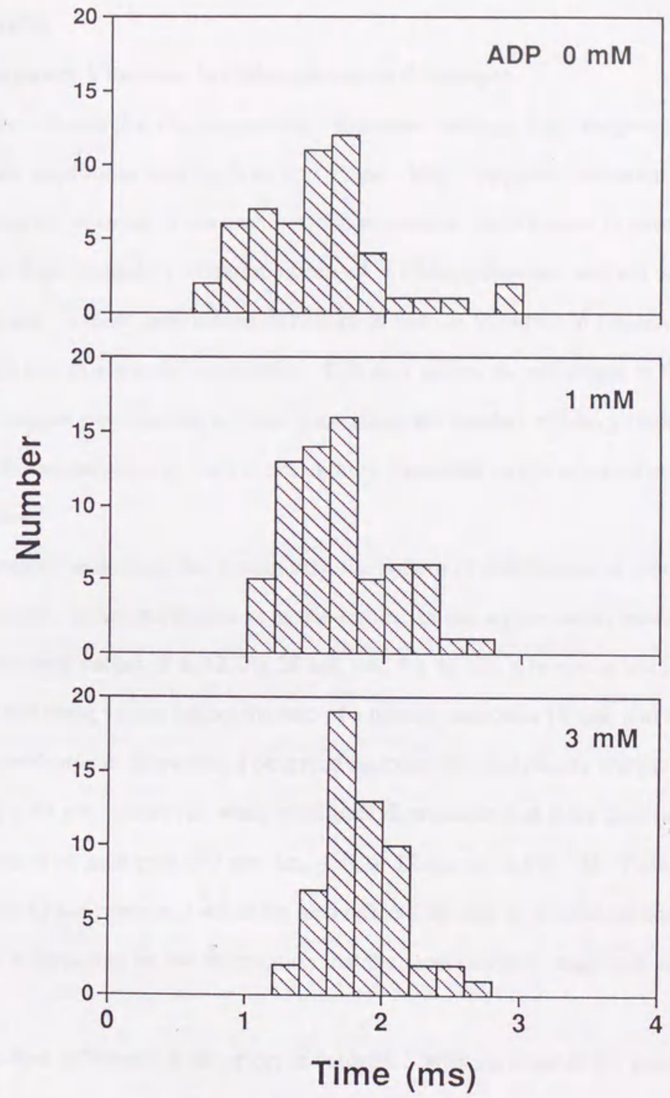

Fig. 13. Histograms of the duration of the descending phase (dt) in the vibration in Fig. 10. The mean value ± standard deviation in 50 measurements for each condition are 1.56 ± 0.47 msec (0 mM ADP), 1.70 ± 0.37 msec (1 mM), and 1.93 ± 0.27 msec (3 mM).

DISCUSSION

High–Frequency Vibration in *Chlamydomonas* Axonemes

I have shown that *Chlamydomonas* axonemes undergo high–frequency vibration at 100–650 Hz with amplitudes ranging from 4 to 40 nm. High–frequency vibration thus seems to be a phenomenon not peculiar to sea urchin sperm axonemes, but common to axonemes in general.

The high–frequency vibration observed in *Chlamydomonas* and sea urchin somewhat differ in detail. A most pronounced difference is that the vibration in *Chlamydomonas* is less regular than that in sea urchin axonemes. This may reflect the difference in the number of dynein molecules participating in force generation, the number of heavy chains in the outer arm (three in *Chlamydomonas* vs. two in sea urchin), axonemal length or axonemal structure between these species.

Possibly because of this irregularity, the pattern of distribution of vibration amplitude in *Chlamydomonas* is not as discrete as in sea urchin. In sea urchin sperm axonemes, the amplitude was found to take values of 4, 12, 20, 28 nm, i.e., 4 + 8n nm, n being an integer. It has been suggested that these values reflect the size of a tubulin monomer (4 nm) and a dimer (8 nm). With *Chlamydomonas* axonemes, I observed no examples that clearly showed multiple peaks at positions 4 + 8n nm. However, when amplitude distribution had more than one peak, peaks were often separated by multiples of 4 nm, i.e., 4, 8, or 12 nm, as in Fig. 7B. Thus, possibly, the amplitude in *Chlamydomonas* vibration also reflects the size of tubulin monomer, 4 nm. This possibility is supported by the observation that the most common amplitude in *pf18* is about 4 nm.

Another difference is the effect of vanadate. While it reduces the vibration amplitude in both species, it increases the frequency in *Chlamydomonas* but not in sea urchin. In the previous study, I postulated that the amplitude of vibration is determined by the balance between the total active force produced by dynein and a presumptive passive elastic force within the axoneme. This is based on the observation that vanadate reduced the vibration amplitude; because vanadate has been shown to produce a kinetic dead–end species (dynein–ADP–vanadate) that interacts

with microtubules only weakly [Shimizu and Johnson, 1983; Vale et al., 1989], vanadate can be regarded as having an activity to reduce the number of active dyneins. If our hypothesis is correct, it is reasonable that vanadate caused an increase in vibration frequency, since reduction of the number of active dyneins will not lower the sliding velocity greatly if friction drag is small, and because vibration with a smaller amplitude at almost the same sliding velocity should result in a higher frequency. The reason why such a frequency increase has not been observed in sea urchin may be that the inhibited dynein–ADP–vanadate species causes some drag. The ATP concentration–dependent variation in amplitude that was observed in *Chlamydomonas* but not in sea urchin sperm may have also originated from difference in properties of dyneins.

Vibration in Dynein Mutants

Mutant axonemes lacking the entire outer arm and those lacking part of the inner arms have been shown to undergo high–frequency vibration. The vibration frequency in the outer–arm mutant *oda1* was about one half of that of the wild type, whereas the frequency as well as the sliding velocity estimated in the inner–arm mutants *ida1* and *ida4* was almost identical with that of wild type (Fig. 6, Table I). These results are reminiscent of the microtubule sliding velocities measured in disintegrating axonemes of wild type and dynein–deficient mutants. Namely, the sliding velocity in *oda1* is as low as about one fifth of the wild–type velocity, whereas that in *ida1* or *ida4* is almost identical (Table I)[Kurimoto and Kamiya, 1991]. The sliding velocity of outer doublets in high–frequency vibration thus appears to be somehow correlated with the velocity measured under load–free conditions.

However, the sliding velocity in the high–frequency vibration, estimated from the frequency–amplitude plots (Fig. 8, Table I), does not support the view that the vibration occurs as a movement in which two counteracting forces simply alternates under load–free conditions. The hyperbolic distribution of plots indicates that the average value of peak–to–peak amplitude (2a) x frequency (f) is 3.2 μm/sec. This suggests that, if the vibration is approximated by a sinusoidal oscillation expressed by $a \cdot \sin(2\pi ft)$, the maximal sliding velocity ($2\pi af$) is

Table I. Sliding Velocities (μm/sec) of Outer Doublets in Wild-type and Mutant Axonemes Estimated in Different Types of Motility

	Species				
Estimated in	*wt*	*ida1*	*ida4*	*oda1*	*pf18*
High-freq. Vibration[a]	10.0	8.4	12.7	ND[b]	5.7
	(4.5–17.3)	(4.5–13.0)	(6.3–20.7)		(3.8–7.9)
Sliding disintegration[c]	18.5	19.0	17.7	4.4	18.3
	(10–24)	(10–24)	(8–26)	(1–10)	(10–24)
Flagellar beating in live cells[d]	15.3	9.5	ND[e]	5.4	—

[a]The maximal velocity in high-frequency vibration estimated by $2\pi af$ using frequency(f) and amplitude(2a) in Fig. 8 (see text). The average value and the range of data (in the parentheses) are shown.

[b]Not measured. I were unable to observe vibration in *oda1* axonemes with poly-lysine coated cover slips.

[c]Measured at 0.5 mM ATP [Kurimoto and Kamiya, 1991]. The data for *ida1* were those measured with *ida2* whose defects and phenotype are identical with those in *ida1*. The data for *pf18* are obtained from measurements with 34 axonemes [E. Kurimoto and T. Yagi, unpublished result]. The average and range of data are shown.

[d]Calculated from Brokaw and Kamiya [1987]. The distance between adjacent doublets in an axoneme is assumed to be 45 nm [Brokaw, 1989].

[e]Not measured. It must be lower than the wild-type value because this mutant displays flagellar beating with an identical beat frequency but with a lower than normal bend angle.

10.0 μm/sec on the average, lower than the sliding velocity in disintegrating axonemes, 18.5 μm/sec (Table I). More direct analyses of the vibration curves, which will be reported elsewhere, also showed that the velocity was variable between 3.5 and 17.0 μm/sec but always lower than the load–free velocity. The possibility that the velocity is only apparently low owing to a loose attachment of microbeads to the axoneme is unlikely, since the vibration amplitude in sea urchin sperm reflected the size of tubulin, indicating that the movement of beads faithfully reflects that of microtubules. The sliding velocity in the sea urchin sperm axoneme has also been estimated to be as low as 5–10 μm/sec [Kamimura and Kamiya, 1992]. Hence these results indicate that microtubules slide considerably more slowly in vibrating axonemes than in disintegrating axonemes.

It is thus somewhat surprising that the sliding velocity estimated in high–frequency vibration is almost identical between wild type and inner–arm mutants and yet lower than the velocity in disintegrating axonemes (Table I). If the lower velocity in high–frequency vibration was due to the presence of a load, the sliding velocity during high–frequency vibration in inner–arm mutants would have been expected to be lower than that in the wild–type axoneme, since it has been shown that the sliding velocity in *ida1* is estimated to be significantly lower than that in wild type when the axoneme is beating, i.e., when the axoneme is subjected to the load of viscous drag and internal elastic force (Table I)[Brokaw and Kamiya, 1987].

This discrepancy may be resolved if I assume that, in high–frequency vibration, the inner–arm dynein works as both an active force generator and an internal drag at the same time; if so, the absence of some inner–arm dyneins may decrease both the power and drag, thus leaving the sliding velocity almost unchanged. As a possible mechanism by which inner arms work as both force generator and drag, I speculate that inner–arm dyneins on two different outer doublets that generate force in opposite directions may counteract in such a way that one row causes a drag upon the movement caused by the other row. However, as an alternative, it is also possible that one subunit of an inner arm dynein produces force while a different subunit binds to the opposite doublet microtubule to create drag. The possibility that different subunits of dynein

behave in such a manner has been suggested with sea urchin outer arm dynein [Moss et al., 1992a, b]. The exact mechanism that brings about the lower sliding velocity in high–frequency vibration is a subject of future studies.

Vibration is Affected by Central Pair/Radial Spokes

A striking observation made in this study is that axonemes of paralyzed mutants *pf18* lacking the central–pair microtubules and *pf14* lacking radial spokes underwent vibration, and did so with significantly lower amplitudes and higher frequencies than in wild–type vibration. This observation indicates that these paralyzed axonemes are not only mechanochemically active, as shown by sliding disintegration experiments [Witman et al., 1978], but also capable of producing oscillatory movements. In addition, it shows that the profile of high–frequency vibration is affected by the internal structure of the axoneme other than dynein itself. This is reminiscent of the observations that the central–pair/radial spoke system affects the axonemal beating [Brokaw et al, 1982] and microtubule sliding in the axoneme [Smith and Sale, 1992], although the true relationship between these and present observations is not understood.

The amplitude–frequency plots for *pf18* axonemes (Fig. 8) yielded estimates of maximal sliding velocities of 3.8–7.9 μm/sec (Table I). These values are much lower than the velocity measured at 0.5 mM ATP in disintegrating axonemes of this mutant (18.3 ± 3.6 μm/sec)(Table I). It is also lower than the sliding velocities estimated in vibrating axonemes of other strains. Why the paralyzed axoneme of *pf18* displays lower amplitude and velocity than other axonemes? One possible explanation is that only a small number of dyneins are active in this mutant, as in the wild type axoneme in the presence of a low concentration of vanadate (Fig. 5). Although I cannot rule out this possibility, I do not think it is highly likely because the ATPase activity in *pf18* axonemes has been found to be as high as that of the wild type (Kagami and Kamiya, unpublished result).

As an alternative hypothesis, I suggest that the low velocity in *pf18* may be due to the simultaneous presence of two populations of dynein arms that produce force in opposite

directions. In other words, I speculate that its low sliding velocity may be due to an incomplete switching between two antagonizing forces produced between two different outer doublets, the incompleteness being much greater than in axonemes of other species. This idea is consistent with our previous assumption that the amplitude is determined by the balance between a presumptive elastic force and the net driving force; the net force now should be the difference between the two antagonizing forces, and thus should be smaller than when only a single row of dynein is active.

Increase in Shear Amplitude Induced by ADP

The amplitude of the hyper–oscillation in *pf18* axoneme significantly increases in the simultaneous presence of ATP and ADP, i.e., under conditions where it can display undulatory movement. The maximal amplitude observed, about 0.1 μm, is close to the shear amplitude in beating axonemes [0.15–0.2 μm; see Brokaw, 1989]. The increase in the oscillation amplitude thus appears to explain the generation of an undulatory movement. In other words, the *pf18* axoneme can not beat under normal conditions possibly because it can not vibrate with a large amplitude; the central–pair microtubules should have a function to increase the shear amplitude. Why the shear amplitude increases at high ADP concentration is not clear. However, the observation that higher ADP concentration results in smoother vibration curve (Fig. 10) suggests that ADP modulates the balance between two antagonizing forces within the axoneme, by somehow suppressing force generation in one direction.

Implications from Asymmetric Oscillation in *pf18* Axonemes

At increased ADP concentrations, some axonemes were found to display hyper–oscillation with an unusually simple asymmetric pattern (Fig. 9b, 9c and 10). Although the vibration curve alone cannot establish the exact mechanism for such a vibration, below I suggest a possible model.

I speculate that the asymmetric oscillation results from a combination of active sliding

between one or two of outer doublets and passive, elastic recoil. The descending phase appears to be driven mostly by an elastic force and, probably to a smaller extent, by an active force generated by dynein. The latter force may be necessary for the generation of the seemingly linear movement in this phase. The reason for postulating an elastic force is that the velocity in the descending phase increases with ADP concentration, as opposed to the movement in general dynein–microtubule sliding interaction, and because the maximal velocity observed (60 μm/sec) is much higher than the maximal velocity observed in disintegrating axonemes [about 20 μm/sec; Kurimoto and Kamiya, 1991]. Thus this vibration curve suggests that the axoneme has an elastic component that can be stretched by as long as 0.1 μm. Such an elastic component has been postulated and named nexin link or inter–doublet link, but there has been no evidence that it actually operates within the axoneme, except that the amplitude of axonemal beating [Brokaw, 1980] or that of hyper oscillation increases upon the elastase digestion of axonemes [Kamimura and Kamiya, 1992]. The present observation provides a strong support for its presence.

The ascending phase, on the other hand, probably is caused by an active shearing movement between dynein and an outer doublet. This is because the observed initial velocity at 0.1 mM ATP (8–15 μm/sec) is comparable to the velocity in outer doublet sliding at the same ATP concentration [10 μm/sec; Kurimoto and Kamiya, 1991]. I suppose that dynein produces a constant force all through the ascending phase and works against an internal elastic load (spring constant k) and viscous drag (frictional constant r). From the balance between the active force F and these forces,

$$F = kx + rv,$$

where x is the displacement from the resting position and v is the velocity of movement. The displacement is then expressed as

$$x = (F/k)\cdot[1-\exp(-k/r\cdot t)],$$

t being the time. This model generates a curve that fits reasonably well with the data of 3 mM ADP in Fig. 10, if I choose values for F/k to be 104 nm and k/r to be 46 x 10^3/sec (Fig. 14). Oiwa and Takahashi [1988] measured the sliding force in sea urchin sperm and obtained results

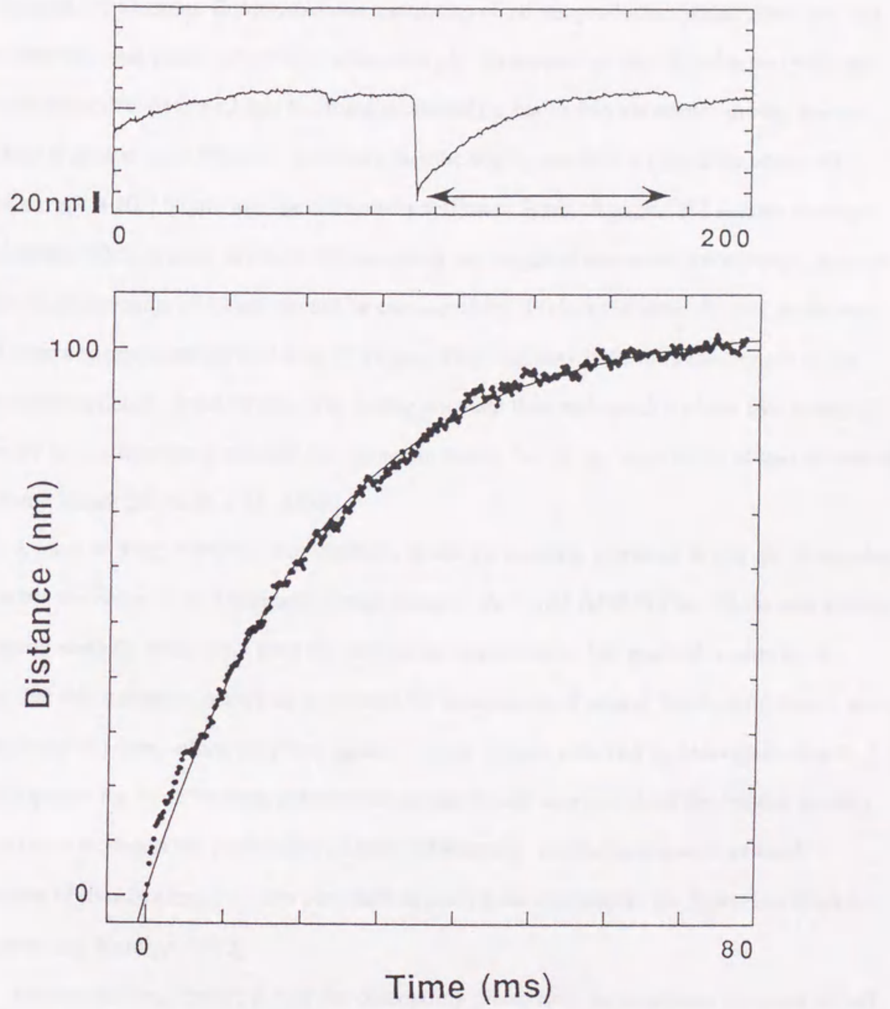

Fig. 14. Curve fitting of the ascending phase with a model. Upper panel, the total view of the recording from which an ascending phase was taken for analysis. Lower panel, experimental data superimposed with a theoretical curve, position = $A \cdot [1-\exp(B \cdot t)]$, A being 104 nm and B being 46 x 10^3/sec. The curve fitting was performed with a nonlinear least–square algorithm. Any ascending phase in the same recording yielded similar values for A and B.

that the force produced is about 40 pN/μm, which is relatively insensitive to the ATP concentration. If I assume *Chlamydomonas* axoneme of 10 μm produces similar force per unit length, then the total force F should be about 400 pN. In support of this, Kamimura (personal communication) has observed that the force produced by sea urchin axonemes during hyper-oscillation is greater than 100 pN. It follows that the spring constant k should be about 400 pN/104 nm = 4 x 10^{-9} N/μm, and the frictional coefficient 9 x 10^{-5} g/sec. If I assume that an inter-doublet link is present at every 100 nm along the length of a doublet, two groups of outer doublets in an axoneme of 10 μm should be connected by 200 links in total. Hence, each link should have a spring constant of 2 x 10^{-11} N/μm. This link may have the same length as the inter-doublet spacing, about 70 nm. The spring constant thus estimated is about two orders of magnitude lower than that estimated for connectin (titin), but of the same order of that of elastin of the same length [Higuchi et al., 1993].

A most striking feature of the vibration in the asymmetric vibration is that the descending phase starts and stops in an extremely abrupt manner. At 3 mM ADP in Fig. 10, the descending phase starts abruptly some time after the ascending displacement has reached a plateau. I suggest that this transition occurs as a cooperative detachment of a large fraction of dynein arms from the outer doublet, which may be triggered by the tension received by individual dynein arms; cooperativity arose because detachment of one dynein arm increases the tension in other arms and thus increases the probability of their detachment. A similar tension-induced detachment of dynein arms has been proposed as part of the mechanism for hyper-oscillation [Kamimura and Kamiya, 1992].

Another striking feature is that the descending phase lasts for an almost constant period of 1.6–1.9 msec. Measurements of this period in other examples yielded similar values: for example, in Fig. 9b, the average ± standard deviation of dt in about 50 measurements each is 1.80 ± 0.46 msec (0 mM ADP), 2.27 ± 0.57 msec (1 mM) and 2.12 ± 0.58 msec (3 mM). It is not clear what this fairly constant time period indicates, but it should be related to the mechanism that abruptly initiates the ascending phase, which must involve a cooperative initiation of the

dynein–microtubule interaction. I speculate that the constant time period may be manifesting a refractory period within which a certain fraction of dynein cannot interact with outer doublets. The mechanism that gives rise to the cooperative initiation of dynein–doublet interaction after a constant period should be an important subject of future studies.

In summary, nanometer–scale motility measurements on *Chlamydomonas* mutant axonemes have thus revealed several unexpected features in flagellar motility. These novel features should be of great significance in considering the mechanism with which the axoneme and dynein function. I hope that our studies on the axonemal movement will further refine measurements on mechanical and chemical changes to molecular levels, and integrate information from different lines of approaches.

ACKNOWLEDGMENTS

I would like to cordially thank Professor Ritsu Kamiya (University of Tokyo) for his guidance and encouragement, without which I would not have been able to complete this work. Dr. Shinji Kamimura (University of Tokyo) gave me invaluable advice on the construction of the apparatus. I am indebted to Dr. Charlotte K. Omoto (Washington State University) who gave me a chance to collaborate on induction of beating in pf mutant axonemes. The joint work provided me with a number of hints on this work.

I am also grateful to Professor Hirokazu Hotani (Nagoya University), Emeritus Professor Sho Asakura (Nagoya University) and the late Professor Yasuo Imae (Nagoya University) for their support, and Dr. Osamu Kagami (National Institute of Bioscience and Human Technology), Dr. Saeko Takada (Nagoya University) and Miss Takako Kato (Nagoya University) for their friendship. Last but not least, I thank all the laboratory members in the Department of Molecular Biology of Nagoya University and in Zoological Institute of University of Tokyo for comfortable research environment I have been enjoying since I entered the graduate school.

REFERENCES

Brokaw, C.J. (1980): Elastase digestion of demembranated sperm flagella. Science 207:1365–1367.

Brokaw, C.J., Luck, D.J.L., and Huang, B. (1982): Analysis of the movement *Chlamydomonas* flagella: the function of the radial–spoke system is revealed by comparison of wild–type and mutant flagella. J. Cell Biol. 92:722–732.

Brokaw, C.J. (1985): Models for oscillation and bend propagation by flagella. In Symposia of the Society for Experimental Biology XXXV, Prokaryotic and Eukaryotic Flagella. W.B. Amos, and J.G. Duckett, editors. Cambridge University Press, Cambridge. 313–338.

Brokaw, C.J., and Kamiya, R. (1987): Bending patterns of *Chlamydomonas* flagella: IV. Mutants with defects in inner and outer dynein arms indicate differences in dynein arm function. Cell Motil. Cytoskel. 8:68–75.

Brokaw, C.J. (1989): Direct measurements of sliding between outer doublet microtubules in swimming sperm flagella. Science 243:1593–1596.

Brokaw, C.J. (1990): Flagellar oscillation: new vibes from beads. J. Cell Sci. 95:527–530

Gibbons, I.R. (1981): Cilia and flagella of eukaryotes. J. Cell Biol. 91:107s–124s.

Gorman, D.S., and Levine, R.P. (1965): Cytochrome F and plastocyanin: their sequence in the photosynthetic electron transport chain of *Chlamydomonas reinhardtii*. Proc. Natl. Acad. Sci. USA. 54:1665–1669.

Harris, E.H. (1988): The *Chlamydomonas* Source Book. Academic press, Inc., San Diego, CA. 780pp

Higuchi, H., Nakauchi, Y., Maruyama, K., and Fujime, S. (1993): Characterization of β–connectin (titin2) from striated muscle by dynamic light scattering. Biophysical J. 65:1906–1915

Huang, B., Ramanis, Z., and Luck, D. J. D. (1982): Suppressor mutations in *Chlamydomonas* reveal a regulatory mechanism for flagellar function. Cell 28:115–124.

Ishijima, S., Sekiguchi, K., and Hiramoto, Y. (1988): Comparative study of the beat patterns of American and Asian horseshoe crab sperm: Evidence for a role of the central pair complex in forming planar waveforms in flagella. Cell Motil. Cytoskeleton 9:264–270.

Kamimura, S., and Kamiya, R. (1989): High–frequency nanometre–scale vibration in 'quiescent' flagellar axonemes. Nature(London). 340:476–478.

Kamimura, S., and Kamiya, R. (1992): High–frequency vibration in flagellar axonemes with amplitude reflecting the size of tubulin. J. Cell Biol. 116:1443–1454.

Kamiya, R. (1988): Mutations at twelve independent loci result in absence of outer dynein arms in *Chlamydomonas reinhardtii*. J. Cell Biol. 107:2253–2258.

Kamiya, R., Kurimoto, E., and Muto, E. (1991): Two types of *Chlamydomonas* flagellar mutants missing different components of inner–arm dynein. J. Cell Biol. 112:441–447.

Kurimoto, E., and Kamiya, R. (1991): Microtubule sliding in flagellar axonemes of *Chlamydomonas* mutants missing inner– or outer–arm dynein: velocity measurements on new types of mutants by an improved method. Cell Motil. Cytoskel. 19:275–281.

Oiwa, K., and Takahashi, K. (1988): The force–velocity relationship for microtubule sliding in demembranated sperm flagella of the sea urchin. Cell Structure and Function 13:193–205.

Moss, A.G., Gatti, J–L., and Witman, G.B. (1992a): The motile β/IC1 subunit of sea urchin sperm outer arm dynein does not form a rigor bond. J. Cell Biol. 118:1177–1188

Moss, A.G., Sale, W.S., Fox, L.A., and Witman, G.B. (1992b): The α subunit of sea urchin sperm outer arm dynein mediates structural and rigor binding to microtubules. J. Cell Biol. 118:1189–1200

Murase, M. (1992): Hyperoscillation of dynein cross–bridge systems. J. Theor. Biol. 154:27–30

Piperno, G., Mead, K. LeDizet, M., and Moscatelli, A. (1994): Mutations in the "dynein regulatory complex" alter the ATP–insensitive binding sites for inner arm dyneins in *Chlamydomonas* axonemes. J. Cell Biol. 125:1109–1117.

Porter, M. E., Knott, J. A., Gardner, L. C. Mitchell, D. R., and Dutcher, S. K. (1994): Mutations

in the SUP–PF–1 locus of *Chlamydomonas reinhardtii* identify a regulatory domain in the beta–dynein heavy chain. J. Cell Biol. 126: 1495–1507.

Smith E.F., and Sale, W.S. (1992): Regulation of dynein–driven microtubule sliding by the radial spokes in flagella. Science 257:1557–1559

Shimizu, T., and Johnson, K.E. (1983): Presteady state kinetic analysis of vanadate–induced inhibition of the dynein ATPase. J. Biol. Chem. 258:13833–13840.

Vale, R.D., Soll, D.M., and Gibbons, I.R. (1989): One–dimensional diffusion of microtubules bound to flagellar dynein. Cell 43:623–632.

Witman, G.B., Plummer, J., and Sander, G. (1978): *Chlamydomonas* flagellar mutants lacking radial spokes and central tubules. Structure, composition, and function of specific axonemal components. J. Cell Biol. 76:729–747.